International Journal of Advancements in Mechanical and Aeronautical Engineering– IJAMAE
Volume 2 : Issue 2 *[ISSN : 2372-4153]*
Publication Date: 19 October, 2015

Thermal-mechanical modeling and analysis of spindle-tapered roller bearing system

Van-Canh Tong and Seong-Wook Hong[#]

***Abstract*— Tapered roller bearing (TRB) has been widely used in rotating machinery because of its high-load-carrying capacity. However, occurrence of high temperature inside TRB, due to the long contact lines between rollers and races and the large sliding friction between roller ends and guide flanges, often becomes a great challenge to utilization of TRB. This paper investigates the thermal behavior of a spindle-TRB system with consideration of rotational speed and radial load. To this end, first, a thermo-mechanical model of rotor-bearing system is developed to provide the frictional heat generation, heat transfer procedure, thermal expansion and transient temperature of the system components. Then, the spindle system thermal behavior is evaluated systematically. Simulation results show the high dependence of temperature on bearing loads, rotational speed. Finally, the steady-state temperature of the system is validated with existing experimental data.**

***Keywords*— tapered roller bearings, thermal expansion, heat generation, induced preload**

I. Introduction

Thermal effect is an essential factor that affects the characteristics of rolling element bearing. This is because increasing temperature leads to the changes in the interaction between races and rolling elements, their material properties, the lubricant viscosity, etc. Therefore, operating temperature obviously plays an important role in the overall performance of whole spindle-bearing system and has been considered by many researchers [1-7]. The thermal problems in TRB are very crucial because of high load and friction between roller and raceways or guide flange. Hence, accurate estimation of temperature in the system containing TRBs is particularly important for providing more useful data for spindle system design such as lubricating and cooling system design, bearing preload mechanism design, bearing seizure prediction, etc.

In this paper, a thermal-mechanical model of a spindle system, composed of a uniform shaft supported by a pair of TRBs, is developed. This model is believed to be applicable for a wide range of practical applications, since the effects of various operation conditions, such rotational speed, radial load, induced preload load on the system temperature are included. Then, both the transient and steady state temperatures of the system components are determined analytically to demonstrate their dependence on the above-mentioned operating conditions. The presented model is finally validated by comparing with an experimental study from Ref. [8].

Van-Canh Tong, Seong-Wook Hong
Kumoh National Institute of Technology
Korea

II. Thermal-mechanical model

A. *Spindle–TRB assembly description*

The thermal behavior of a spindle-TRB system as indicated in Fig. 1 was analyzed. TRBs of Timken 4595/4536 are utilized in this study. The SAE 20 lubricant oil is used for the system lubrication by using the oil bath method. The rotational speed of shaft is chosen from 1,000 to 4,000 rpm. The radial load on each bearing is varied from 5,000 N to 10,000N. The thermal mechanical properties of the system components are listed in Table I.

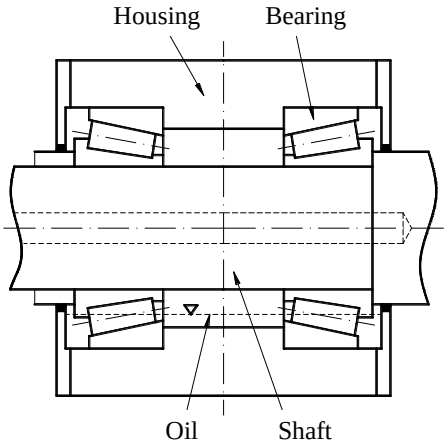

Figure 1. Spindle-TRB system.

TABLE I. THERMAL MECHANICAL PROPERTIES OF THE SYSTEM COMPONENTS

Component	Bearing	Shaft	Housing
Material	SUS440C	SC45	FC200
E (MPa)	200,000	207,000	98,000
α (10^{-6}/°C)	10.1	12.8	10.4

B. *System block diagram*

Fig. 2 shows the entire closed-loop block diagram which consists of 4 stages: friction heat generation, heat transfer, thermal expansion, and thermally induced preload. In the first stage, the frictional heat generation in bearing is calculated as the input value for determination of the system temperature in the second stage. The thermal expansion of components is calculated in the third stage. In the last stage, a bearing model is used to estimate the induced preload based on the change of interaction between the roller and the races. The induced preload is then updated as the external load back at the first stage for starting a new iteration cycle.

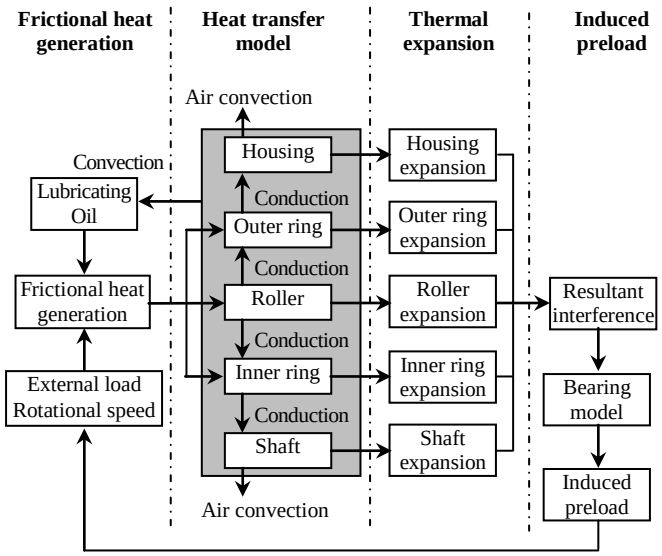

Figure 2. Block diagram of the model.

C. Heat generation computation

The total friction heat in a bearing is calculated by [1]:

$$\dot{H}_f = \frac{Mn}{9550} \tag{1}$$

where n and M are the rotational speed and total friction torque of TRB, respectively. In general, the bearing friction torque composes of three components: i.e.

$$M = M_l + M_v \tag{2}$$

where M_l and M_v represent the load and viscous friction torques, respectively. The friction torque due to the applied load to TRB is calculated as

$$M_l = f_1 P_1 d_m \tag{3}$$

where f_1 = 0.0004 is the bearing load factor. d_m denotes the bearing pitch diameter. The load P_1 depends on the applied load on the bearing and can be represented by

$$P_1 = 1.21 Y F_z \tag{4}$$

or

$$P_1 = F_x \tag{5}$$

where F_z and F_x represent the axial and radial loads of bearing. Y is the radial load factor that is equal to 1.7 for the current TRB. The larger value between (4) and (5) will be used for P_1.

The viscous friction torque can be determined by [1]

$$M_v = 10^{-7} f_0 (\nu n)^{2/3} d_m^3, \nu n \geq 2000 \tag{6}$$

$$M_v = 160 \times 10^{-7} f_0 d_m^3, \nu n < 2000 \tag{7}$$

The coefficient factor f_0 depends on the bearing types and lubrication method. In the current study, f_0 = 3 with referring to [9]. ν represents the kinematic viscosity of lubricant.

D. Heat transfer model

As illustrated in Fig 3, a set of 13 nodes is used for prediction of system temperature. The inside of the housing is assumed to be covered with lubricant in the oil bath so as to be described by a single temperature node 6. The TRB inner ring, roller and outer ring are modeled by lumped thermal masses and indicated by temperature nodes 7, 8 and 9, in which a component is assumed to have an identical temperature and connects to each other by a thermal constriction resistance, as proposed by Winer [3]. The housing and the shaft temperature are described by seven nodes connected to the network by thermal resistance.

For each node of the thermal network, the overall equation for heat balance can be written as:

$$\dot{H}_{in} + \dot{H}_g + \dot{H}_{out} = mc\frac{\partial T}{\partial t} \tag{8}$$

where $\dot{H}_{in}$ and $\dot{H}_{out}$ are the inlet and outlet heat rate, respectively. $\dot{H}_g$ represents the heat generation. m is the mass of control volume represented by the node and c is the specific heat of material. By applying (8), the heat balance equation for the roller (node 8) can be obtained as

$$\frac{T_7 - T_8}{R_{e1}} + \frac{T_9 - T_8}{R_{e2}} + \frac{T_6 - T_8}{R_v} + \dot{H}_{fr} = m_8 C_8 \frac{\partial T_8}{\partial t} \tag{9}$$

where R_v is the convective resistance associated with the contact between the lubricant and roller. T_7, T_9, T_8 and T_6 are the temperatures of inner ring, outer ring, roller and oil, respectively. $R_{e1,2}$ represent the thermal constriction resistance related to the roller in contact with the inner and outer ring.

The heat balance equation for inner and outer ring (nodes 7 and 9) can be expressed as, respectively

$$\frac{T_4 - T_7}{R_{t1}} + \frac{T_8 - T_7}{R_{e1}} + \frac{T_6 - T_7}{R_v} + \dot{H}_{fi} = m_7 C_7 \frac{\partial T_7}{\partial t} \tag{10}$$

$$\frac{T_{10} - T_9}{R_{t2}} + \frac{T_8 - T_9}{R_{e2}} + \frac{T_6 - T_9}{R_v} + \dot{H}_{fo} = m_9 C_9 \frac{\partial T_9}{\partial t} \tag{11}$$

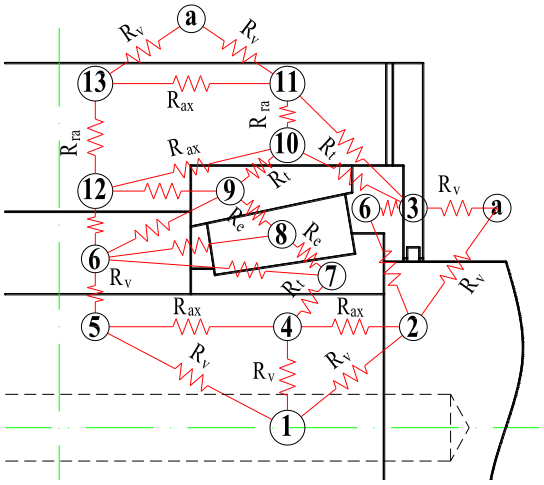

Figure 3. Network of temperature nodes for TRB.

where T_4 and T_{10} are the temperatures of the corresponding nodes 4 and 10. $R_{t1,2}$ are the thermal contact resistance between the inner race and shaft, and the outer race and housing. $\dot{H}_{fr}, \dot{H}_{fi}$ and $\dot{H}_{fo}$ are the fractions of friction heat distributed to the roller, inner ring and outer ring, respectively. Assume that the friction heat is equally distributed over the roller and races [2], hence:

$$\dot{H}_{fr} = 0.5\dot{H}_f \tag{12}$$

$$\dot{H}_{fi} = \dot{H}_{fo} = 0.25\dot{H}_f \tag{13}$$

Using the similar concept presented in (8)-(11), a set of 13 equations, corresponding to all temperature nodes, can be obtained. The only difference among the equations is the selection of appropriate thermal resistance associated with each pair of elements, which will be discussed in the next section. The iterative Newton-Raphson method is further used to iteratively solve the system of non-linear equations. Because the lubricant viscosity, which appears in (6) and (7), varies with regard to temperature, the viscosity of lubricant should be updated at each iteration. From the discrete experiment values of lubricant viscosity and corresponding temperature [10], the appropriate viscosity at a certain temperature can be determined by an interpolation method.

E. *Thermal resistance of the system*

Thermal resistance of the system can be categorized into four groups depending on the heat transfer characteristics. The first group is the thermal constriction resistance between rollers and raceways. The thermal constriction resistance of a single roller is calculated as [3]

$$R_s = 2\frac{0.478}{L\sqrt{a}\sqrt{\rho c k}\sqrt{V}} \tag{14}$$

where L and a are the length of contact perpendicular to the motion direction and the width of the contact in the direction of motion, respectively. ρ and k represent the density and thermal conductivity. V is the surface speed at the contact. With z loaded rollers forming a parallel resistance circuit against radial heat flow, the equivalent thermal constriction resistances by the roller and races are:

$$R_{e1,2} = \frac{R_{s1,2}}{z} \tag{15}$$

The second group is the thermal convective resistance between the lubricant or ambient air and the surface of system components.

$$R_v = \frac{1}{h_v S} \tag{16}$$

where h_v is the film coefficient of heat transfer. For the heat transfer by convection from lubricant, h_v is determined by [1]

$$h_v = 0.332k\,\mathrm{Pr}^{1/3}\left(\frac{u_s}{\nu x}\right)^{1/2} \tag{17}$$

where u_s and x are equal to one third of cage velocity and housing diameter, respectively. Pr is the Prantl number

$$\mathrm{Pr} = \frac{\nu}{\alpha} \tag{18}$$

Regarding the heat transfer between the ambient air and housing external surface, h_v depends on the housing structure, the surrounding air velocity, etc. In this study h_v is approximated by 25 W/m^{2}K in the case of quiescent air and natural convection in according with Incropera [11].

The third group includes the radial conductive R_{ra} (e. g, $R_{10\text{-}11}$, $R_{12\text{-}13}$) and the axial conductive resistances of shaft and housing R_{ax} (e. g, $R_{2\text{-}4}$, $R_{4\text{-}5}$, $R_{11\text{-}13}$, $R_{10\text{-}12}$) expressed by, respectively:

$$R_{ra} = \frac{\ln(R_o/R_i)}{2\pi k W} \tag{19}$$

$$R_{ax} = \frac{\Delta L}{kS} \tag{20}$$

where S and ΔL are the area that is normal to the heat flow and the distance between the two nodes, respectively. R_o, R_i and W represent the outer radius, inner radius and width of the annular structure in which heat flow occurs [1].

The last group is the thermal contact resistances, which is calculated by [11]:

$$R_t = \frac{1}{h_c S} \tag{21}$$

where h_c is the conductance contact coefficient. The values for shaft-inner race and outer race-housing conductance contact coefficient are estimated as 7680 W/m^{2}K and 500 W/m^{2}K, respectively, by using the equations from Min et al. [12].

F. *Thermal expansion of the system*

Under thermal growth, the roller, inner and outer races are expanded radially by δ_r, δ_{in} and δ_{out}, while the shaft and the housing are axially expanded by ε_s and ε_h, respectively. Hence, the total radial and axial interference changes are:

$$\delta = \delta_r + \frac{\delta_{in} - \delta_{out}}{2} \tag{22}$$

$$\varepsilon = \frac{\varepsilon_h - \varepsilon_s}{2} \tag{23}$$

The radial expansion of the inner ring or the outer ring is calculated by:

$$\delta = \alpha r \Delta T \tag{24}$$

where α, r and ΔT represent the thermal expansion coefficient, radius and temperature increment, respectively.

Because the temperature varies along the shaft or the housing, the total axial expansion of the shaft or the housing is the summation of axial expansion of each individual part. Thermal expansion of an arbitrary part is calculated by

$$\varepsilon_h = \left(\frac{2\alpha_h}{r_{ho}^2 - r_{hi}^2} \int_{r_{hi}}^{r_{ho}} T_h r_h dr_h \right) l_h \quad (25)$$

$$\varepsilon_s = \left(\frac{2\alpha_s}{r_{so}^2} \int_{0}^{r_{so}} T_s r_s dr_s \right) l_s \quad (26)$$

By assuming that the temperatures in radial direction of shaft and housing are linear, the housing and shaft axial expansion in (25) and (26) can be easily obtained.

G. *Bearing model*

Fig. 4 briefly describes the entire bearing model. From the resultant interference, the induced preload can be determined as follows. First, the displacement of inner ring at each roller location is calculated. Subsequently, by assuming the roller displacement, the contact load between a roller and races are determined. The roller equilibrium equation is then solved by considering the effects of centrifugal force and gyroscopic moment. The undated value of roller displacement is compared to the initial guess for the convergence decision. Finally, after all the roller displacements are available, the induced preload can be directly computed from the equilibrium condition of the whole bearing [13].

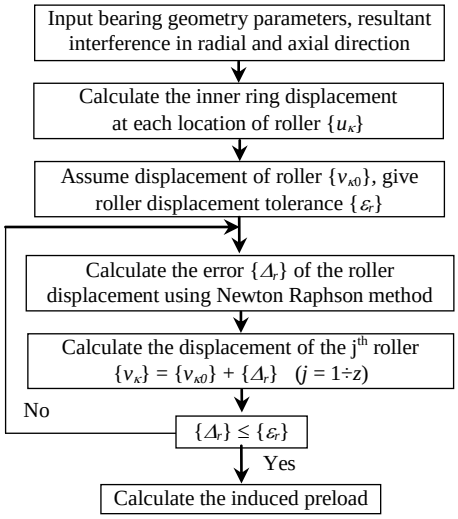

Figure 4. Calculation model for thermally induced preload in TRB.

III. RESULTS AND DISCUSSION

Simulation is carried out with the presented thermal-mechanical model. The effects of rotational speed, radial load on the thermal behavior of the spindle system are discussed. Finally, the computational results are compared with those from an experimental study in [8].

A. *Rotational speed effects*

The rotational speed of spindle is selected from 1,000 to 3,500 rpm while the radial load is kept constant at 4,000 N. Fig. 5(a) shows the effect of rotational speed on the temperature of bearing outer race. It can be observed that the temperature rapidly increases right after the motor starts up. Then, the temperature moderately increases and becoming settled down after about 2.5 hours where the system reaches a steady state condition. While the frictional torque increases quickly from 0 to its maximum value as shown in Fig. 5(b), the frictional torque continues to decrease slowly due to the reduction of lubricant viscosity with regard to the oil temperature. Fig. 6 shows the thermal behavior of outer race during the so-called step test, which represents that the spindle initially runs at a constant speed of 2,000 rpm and coasts down the motor after 2 hours. In this case, the temperature straightforwardly goes up and then drops to reach the steady state condition after the speed changes.

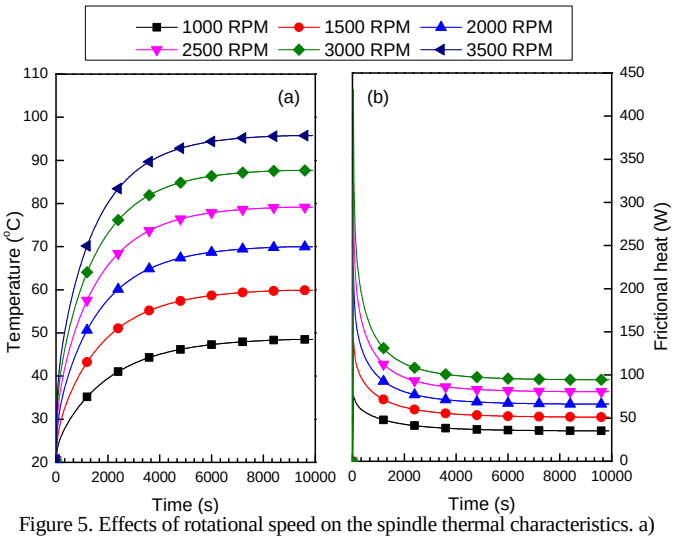

Figure 5. Effects of rotational speed on the spindle thermal characteristics. a) Bearing outer race temperature, b. Frictional heat generation (F_x = 4,000 N).

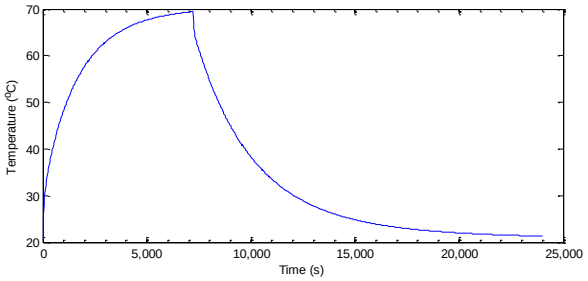

Figure 6. Outer race temperature variation during step test (F_x = 4,000 N; n = 2,000 rpm).

B. *Radial load effects*

System temperature is evaluated under the radial load varying from 5,000 to 10,000 N while the speed remains constant at 2,000 rpm. Fig. 7 shows the variation of bearing outer race temperature and frictional heat with the increase of radial load. In this case, a similar variation trend can be found as the thermal-speed dependence shown in Fig. 5. However, it can be seen that the effects of rotational speed on the system temperature and heat generation are higher compared to the radial load. This could be due to the fact that the viscous friction torque has a foremost contribution. Moreover, the steady state temperature shows an approximately linear relationship with radial load when the temperature increment is almost 3 degree with increasing radial load from 5,000 to 10,000 N. A similar behavior has been also reported earlier for the deep groove ball bearings [6].

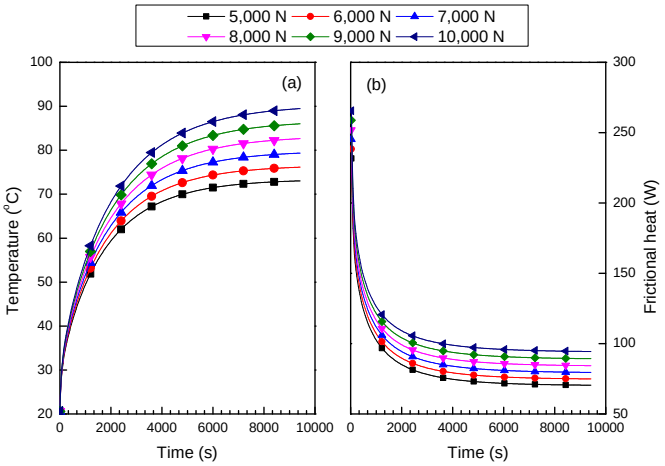

Figure 7. Effects of radial load on the spindle thermal characteristics. a. Outer race temperature, b. Frictional heat generation (n = 2,000 rpm).

C. *Experimental comparison*

In this section, the computation results are compared with those of experimental data in Ref. [8] under the steady state condition. The test in Ref. [8] was carried out with a constant radial load of 4,000 N and the rotational speed from 1,000 to 4,000 rpm. Table 2 shows the comparison of the computational and experimental temperatures at several nodes of the spindle system under the radial load of 4,000 N and the rotational speed of 4,000 rpm. From Table II, an overall agreement can be seen between simulation and experiment. The estimated oil temperature is believed to be less accurate, primarily due to the difficulties in describing the heat convection within the housing [1].

TABLE II. COMPARISION BETWEEN SIMULATION AND EXPERIMENT

Node	4	5	6	7	9	10	11
Experiment (°C)	104.0	102.0	89.0	106.0	105.0	101.0	90.6
Simulation (°C)	103.4	103.0	102.5	103.8	103.4	96.1	94.8

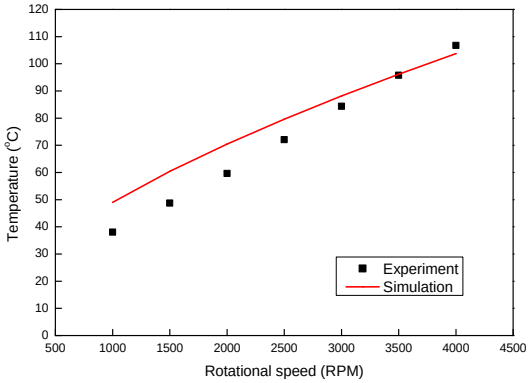

Figure 8. Comparison of simulation and experiment for steady state temperature of the inner race (F_x = 4,000 N, n = 4,000 rpm).

Fig. 8 demonstrates the steady state temperature of inner race as a function of rotational speed. The computational temperatures are fairly well matched with those from experiment. Both simulation and measurement temperatures show a nearly linear relationship with regard to rotational speed as addressed before. It should be noted that the experimental temperatures increase somehow faster than those of computation. This could be due to the inaccurate information in thermal-mechanical properties of the spindle system components. The materials used for the current study, as listed in Table 1, were not described well in Ref. [8].

IV. CONCLUSIONS

A thermal behavior of a spindle–TRB system has been investigated in consideration with the effects of rotational speed and radial load. The computational results are obtained by using a thermal-mechanical model to investigate the steady state condition, as well as the transient temperature. The model is verified by means of comparing with existing experimental data. The beneficial aspect of the current model is the general model with taking into account almost all factors, such as the thermal expansion, induced preload, viscous and load friction torque, heat generation, radial load and speed effects. It is believed that the developed model is applicable for further thermal investigation of spindle with different configurations and/or operating conditions, e.g., spindles with more than two bearings and different bearing configurations, spindles with circulating lubrication system.

Acknowledgment

This research was financially supported by the Korea Institute of Machinery and Materials.

References

[1] T. A. Harris, Rolling Bearing Analysis, 4th ed., John Wiley & Sons, New York, 2001.

[2] F. C. Pruvot, “High speed bearings for machine tool spindles,” Annals of the CIRP, Vol.29, pp. 293-297, 1980.

[3] W. O. Winer, S. Bair, and B. Gecim, “Thermal-resistance of a tapered roller bearing,” ASLE Trans., Vol. 29, pp.539-547, 1986.

[4] J. L. Stein, and J. F. Tu, “A State-space model for monitoring thermally-induced preload in antifriction spindle bearings of high-speed machine tools,” J. Dyn. Sys. T-T ASME, Vol. 116, pp. 372-386, 1994.

[5] B. Bossmanns, and J. F. Tu, “A Power Flow Model for High Speed Motorized Spindles-Heat Generation Characterization,” J. Manuf. Sci. E-T ASME, Vol. 123, pp. 494-505, 2000.

[6] J. Takabi, and M. M. Khonsari, “Experimental testing and thermal analysis of ball bearings,” Tribol. Int., Vol. 60, pp. 93-103, 2013.

[7] K. Nakajima, “Thermal contact resistance between balls and rings of a bearing under axial, radial, and combined loads,” J. Thermophys. Heat. Tr., Vol. 9, pp. 88-95, 1995.

[8] V. A. Schwarz, “ Experimental studies on the thermal behavior of a tapered roller bearing assembly,” Proceedings of the 11th Brazilian Congress of Thermal Sciences and Engineering, Rio de Janeiro, 2006.

[9] ISO: 15312-2003(E), Rolling bearings-Thermal speed rating-Calculation and coefficients, International Organization for Standardization, 2003.

[10] TMEC®, www.tmec.com/attachments/contentmanagers/331/sae20.gif, Mechanical Equipment Company, (Accessed date: Oct 24, 2010).

[11] F. P. Incropera, and D. P. De Witt, Fundamentals of heat and mass transfer, 4th ed., John Wiley and Sons, 1996.

[12] X. Min, J. Shuyun, and C. Ying, “An improved thermal model for machine tool bearings,” Int. J. of Mach. Tool. Manu., Vol. 47, pp. 53-62, 2007.

[13] V. C. Tong, and S. W. Hong, “Characteristics of tapered roller bearing subjected to combined radial and moment loads,” Int. J. Precis. Eng. Manuf.-Green Tech., Vol. 1, pp. 323-328, 2014.